PERGAMON

Journal of Structural Geology 25 (2003) 441–453

JOURNAL OF STRUCTURAL GEOLOGY

www.elsevier.com/locate/jsg

Magnetic fabrics in the Cabanas Granite (NE Brazil): interplay between emplacement and regional fabrics in a dextral transpressive regime

Sérgio P. Neves[a,*], Alexandre M.B. Araújo[a], Paulo B. Correia[b], Gorki Mariano[a]

[a]*Departamento de Geologia, Universidade Federal de Pernambuco, 50740-530 Recife, Brazil*
[b]*Departamento de Engenharia de Minas, Universidade Federal de Pernambuco, 50740-530 Recife, Brazil*

Received 19 September 2000; received in revised form 3 December 2001; accepted 5 December 2001

Abstract

The late Neoproterozoic Cabanas Granite, northeastern Brazil, is a tabular body that was emplaced south of the dextral East Pernambuco shear zone system. Anisotropy of magnetic susceptibility (AMS) measurements reveal that the Cabanas Granite has fabric patterns more complex than usually reported in plutons intruded in similar settings. Most structures have EW- to ENE-trending magnetic lineations consistent with the overall regional structural direction. In the north, these structures parallel the mylonitic fabric encountered in shear zones that bound or cross-cut the pluton. In the central and southern portions of the pluton, magnetic foliation trajectories, the overall banded disposition of the iso-susceptibility lines, and shape parameters of the AMS ellipsoids suggest that the Cabanas Granite was subjected to ENE-trending folding, along with its underlying and enclosing country rocks. It is concluded that emplacement took place during regional dextral transpression. A secondary, but well-developed, family of structures consists of N- to NW-plunging lineations, which is interpreted to represent the trace of the vertical conduits that fed the pluton. This study emphasizes the utility of the AMS to unravel both the internal structure of low anisotropy plutons and the interplay between emplacement and regional straining during magma crystallization.

Keywords: Anisotropy of magnetic susceptibility (AMS); Pluton emplacement; Transpression

1. Introduction

Several processes lead to the development of magmatic structures in granitoids. These include convection in a magma chamber, crystal settling, flow of magma during ascent and emplacement, ballooning, and tectonic deformation of an incompletely solidified pluton (see review in Paterson et al., 1998). Given that different processes may produce sets of structures with quite distinct orientations and geometries, it is surprising that composite fabrics in granite plutons are not more frequently reported in the literature. However, coexisting fabric patterns have been described in a growing number of studies of granitoid bodies. Commonly reported situations are the occurrence of (a) subvertical linear fabrics in restricted areas of a pluton that exhibits dominantly subhorizontal fabrics (e.g. Vigneresse and Bouchez, 1997; McNulty et al., 2000), and (b) planar and/or linear fabric elements with oblique orientations, such as corridors of subvertical foliations bearing shallowly plunging lineations at high angles to the strike of shallowly to moderately dipping foliations (Archanjo et al., 1994; Bouchez and Gleizes, 1995; Gleizes et al., 1998; Yenes et al., 1999). In the first case, areas with steeply plunging lineations, especially where associated with negative gravity anomalies, are interpreted as feeder zones, whereas the subhorizontal lineations are interpreted to track the flow of magma as it spreads at its emplacement level (Améglio et al., 1997). In the second situation, overprinting of an older foliation, developed during early emplacement or later in the magma chamber, by a foliation of tectonic origin, resulting from deformation of the pluton before full crystallization, is commonly invoked (Neves et al., 1996; Benn et al., 1998).

We report the case of the Cabanas Granite, northeastern Brazil, emplaced and deformed in a dextral transpressive strike-slip setting, which shows two almost orthogonal fabrics. A former family of structures clearly records pre-full crystallization deformation related to the transpressive regime, but the second set cannot be simply ascribed to wrenching. We discuss the reason why two fabrics were produced and preserved in this case, since plutons emplaced in similar settings worldwide are typically characterized by a dominant subvertical foliation bearing a subhorizontal lineation (e.g. Hutton, 1982; McCaffrey, 1992; Ferré et

* Corresponding author. Tel.: +55-081-32718240; fax: +55-081-32718234.
E-mail address: serpane@hotlink.com.br (S.P. Neves).

0191-8141/03/$ - see front matter © 2002 Elsevier Science Ltd. All rights reserved.
PII: S0191-8141(02)00003-2

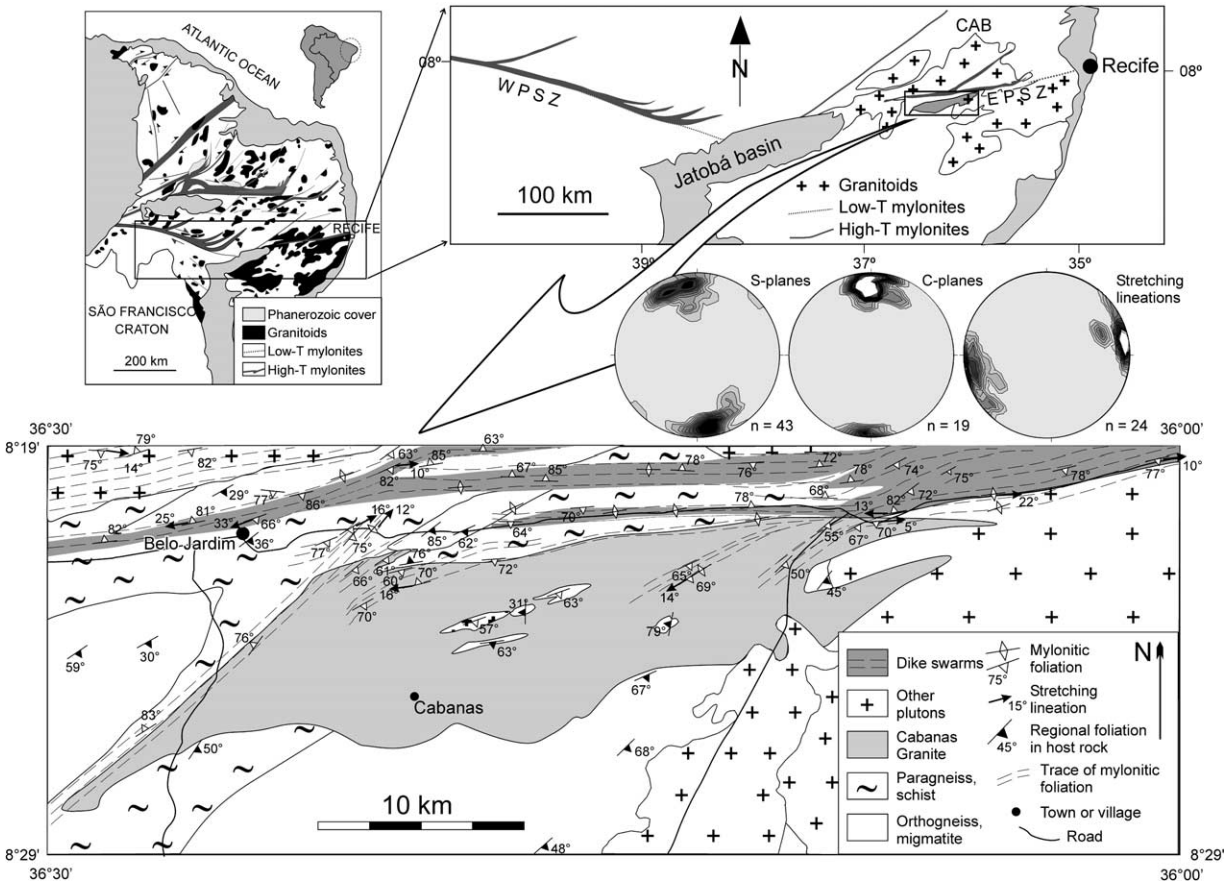

Fig. 1. Location and geological map of the Cabanas Granite. CAB: Caruaru–Arcoverde batholith, WPSZ: Western Pernambuco Shear Zone, EPSZ: Eastern Pernambuco Shear Zone. Stereograms are lower hemisphere Schmidt projections of contoured poles to planes and linear data collected from the EPSZ in the studied area.

al., 1995). Using information gathered from the pluton and the wall rocks we propose a model for its emplacement and deformation. Finally, the implications of this study for the interpretation and significance of magmatic fabrics in granites in general are considered. A penetrative fabric is not discernible in most outcrops of the Cabanas Granite and the unraveling of the two fabric patterns was only possible through an anisotropy of magnetic susceptibility (AMS) study, attesting the usefulness of this technique to the structural investigation of plutonic rocks.

2. Geological setting

The Cabanas Granite, approximately 40 × 8 km in size, is an ENE-trending, elongate pluton located immediately to the south of the East Pernambuco shear zone system (EPSZ). The EPSZ is one of the several transcurrent shear zones that cross-cut the Neoproterozoic Borborema Province and characterize the Brasiliano/Pan-African orogeny in northeastern Brazil (Vauchez et al., 1995) (Fig. 1). Structural, kinematic and geochronological work conducted on shear zones in the central sector of the Borborema Province, including the EPSZ, show that they mainly developed at high temperatures (>600 °C), with local migmatization coeval with transcurrent shear, around 590–550 Ma (Vauchez and Egydio-Silva, 1992; Vauchez et al., 1995; Corsini et al., 1998; Neves and Mariano, 1999; Guimarães et al., 2000; Neves et al., 2000; Silva and Mariano, 2000). Subsequent deformation at greenschist facies conditions is restricted to narrow, less than 1 km wide, belts.

Fig. 2. Field photographs illustrating outcrop relations in the Cabanas Granite. Arrow heads point to the north. Pen in (a), (c) and (d) is 15 cm long. (a) Gneiss–granite contact in the southeast portion of the Cabanas Granite. The contact strikes NS and the gneissic banding dips steeply to the northwest, being cross-cut by N20°E sinistral shear bands (highlighted by dashed lines). (b) Stromatitic migmatite displaying Type 3 interference fold pattern cross-cut by NW–SE dyke of leucogranite. (c) Mylonitic coarse-grained granite showing EW-striking *C*-type shear bands cross-cut by NW-striking, contorted and NE-striking, planar dikes of leucogranite. (d) Contorted dike of leucogranite in mylonitic orthogneiss indicating post-emplacement deformation. (e) Leucogranite veins parallel to axial planes of NE–SW-trending folds in mylonitic orthogneiss. The veins are interpreted as dikes emplaced at high angle to the mylonitic, ENE-trending mylonitic foliation that rotated synthetically during progressive inhomogeneous non-coaxial dextral shearing.

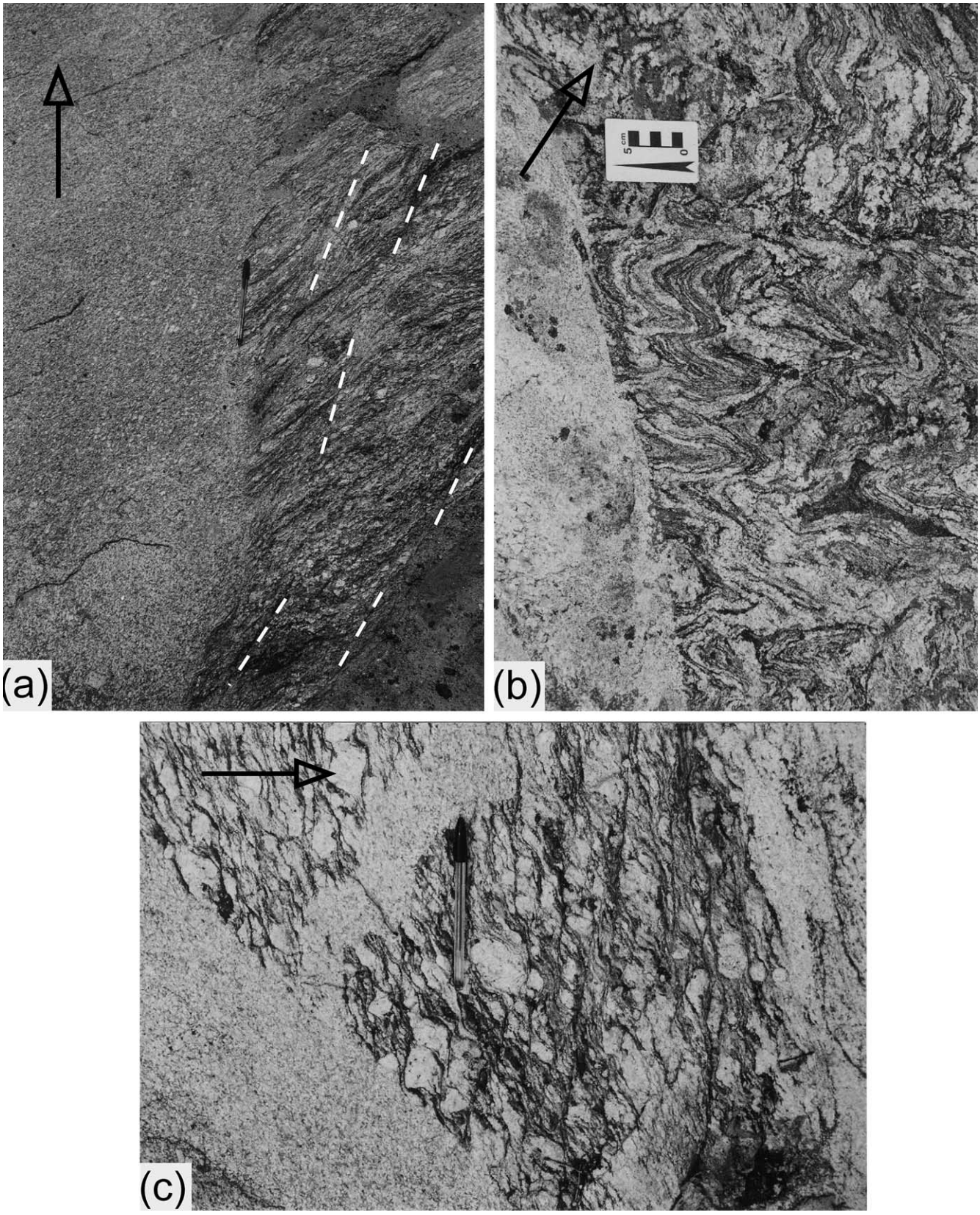
(a)
(b)
5 cm
0
(c)

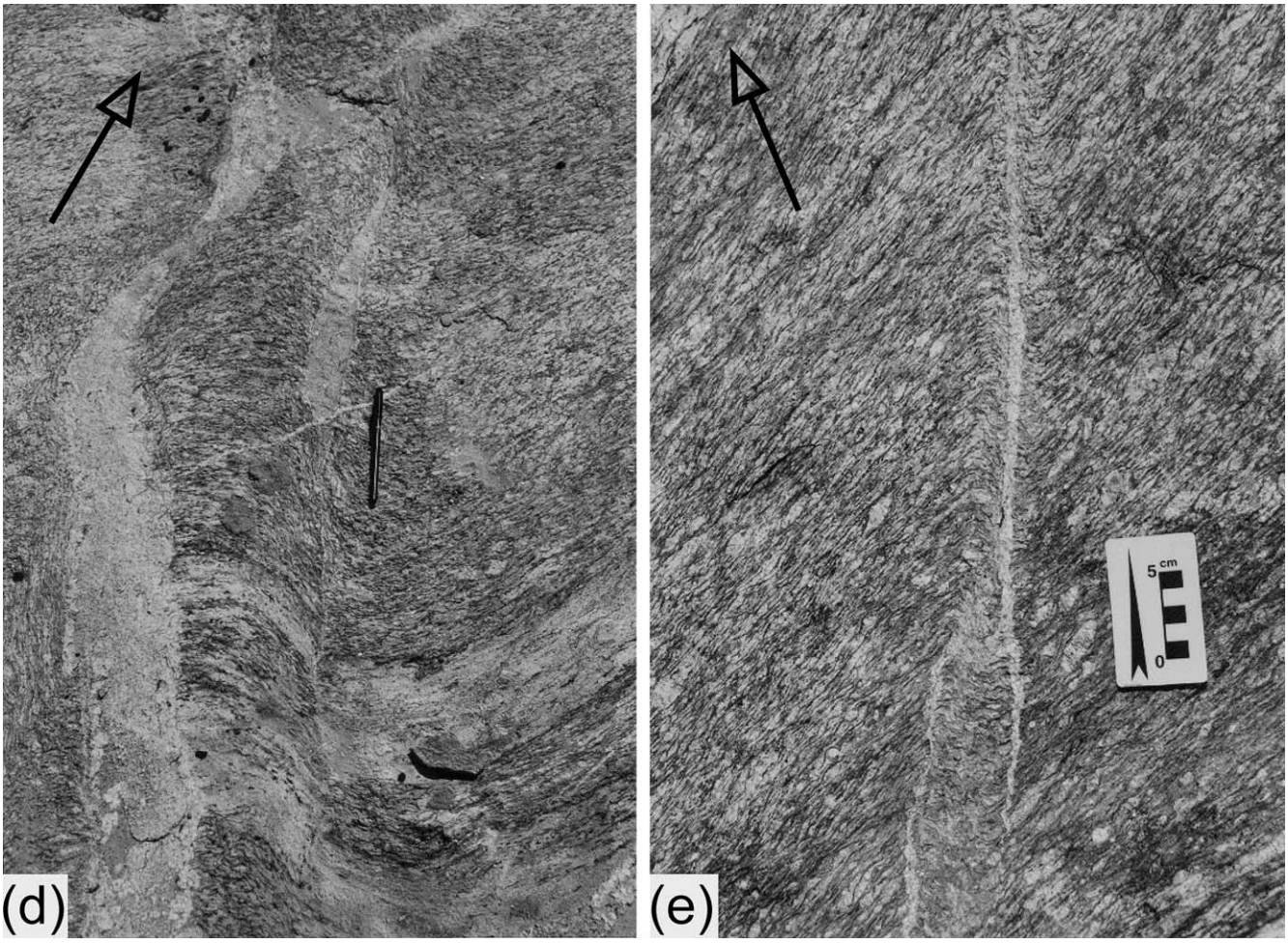

Fig. 2. (*continued*)

The EPSZ consists of two high-temperature mylonitic belts located at the southern border of the Caruaru–Arcoverde batholith (Fig. 1), and of several low-temperature belts of overlapping right-stepping shear zones to the south and east of these (Neves and Mariano, 1999). The mylonite protoliths in the low-temperature belts are dominantly magmatic rocks (mainly syenites, monzonites, diorites and leucogranites) derived from dike swarms. In the study area, a southern segment of the EPSZ is located at the northern contact of the Cabanas Granite, and two subsidiary shear zones cross-cut the granite body in its eastern part (Fig. 1).

The country rocks of the Cabanas Granite along its northern and northwestern contacts are orthogneisses, biotite schists, paragneisses and minor calc–silicate rocks, while orthogneisses and migmatites dominate to the south of the pluton (Fig. 1). To the east, the Cabanas Granite intrudes a biotite ± amphibole medium- to coarse-grained granite batholith. The biotite–sillimanite–garnet assemblage in the micaschists indicates a regional metamorphism at amphibolite facies condition. The metamorphism is correlated with a low-angle, non-coaxial shearing event, with a top-to-the-NE sense of displacement, which developed a foliation parallel to the compositional banding (Neves et al., 2000). In the studied area, the regional foliation is characterized by NE–SW-strikes and moderate dips to the southeast. Repetition of lithological units to the north of the Cabanas Granite (Fig. 1) calls for the existence of NE-striking map-scale folds, consistent with field observations of upright to inclined folds with this direction. Deformation of the country rocks by transcurrent shear was limited, and in general not enough to produce mylonitic fabrics. Shearing was mainly localized at the southern border of the Caruaru–Arcoverde batholith, at the northern border of the Cabanas Granite, and in dike swarms (Fig. 1). These observations are consistent with partitioning of strain into components of strike-slip shearing and NW–SE shortening during transpression.

Exposed contacts of the Cabanas Granite with the country rocks are sharp. The undeformed southern contact is observed to cross-cut locally the migmatite/gneiss banding. To the southeast, the gneissic banding is affected by ENE-trending sinistral shear bands and also cross-cut by the granite (Fig. 2a). Kilometer-long xenoliths of both non-mylonitic and mylonitic varieties occur in the pluton (Fig. 1). The non-mylonitic xenoliths are mostly made of folded stromatitic migmatites that may record two fold events.

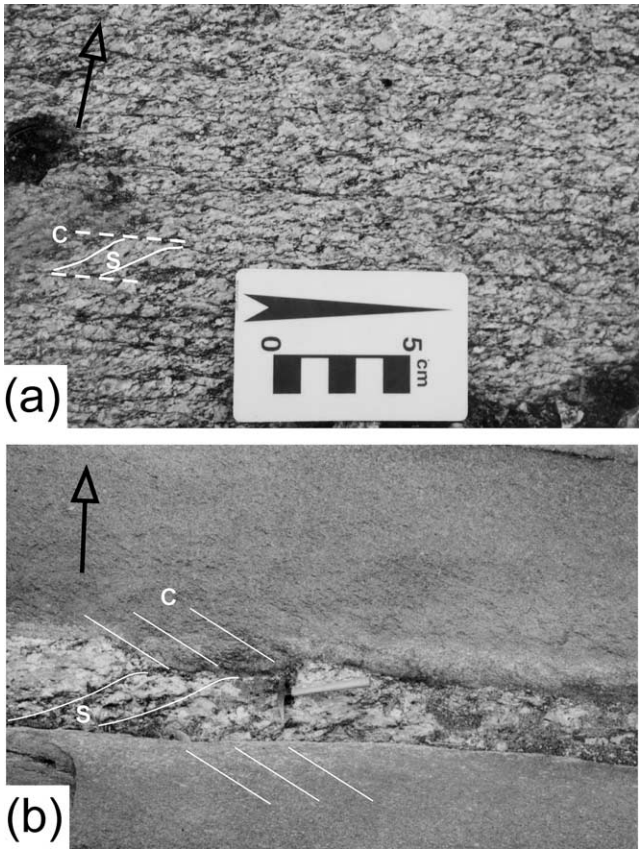

Fig. 3. Outcrop-scale deformation aspects of the Cabanas Granite. Arrow heads point to the north. (a) *S–C* fabric indicating dextral shear in mylonitic leucogranite from the northern part of the pluton. (b) Pegmatite dike displaying mylonitic foliation (parallel to hammer) in deformed leucogranite. *C*-type shear bands run from top left to lower right in the granite. Hammer is 32 cm long.

Dikes of leucogranite with NW–SE strikes truncate the ENE- to NE-trending axial planes of folds of the latter fold event (Fig. 2b). The mylonitic xenoliths derive from porphyritic granites, which are petrographically similar to rocks of the Caruaru–Arcoverde Batholith, and orthogneisses. They show a well developed, mylonitic *S–C* fabric formed at high-temperature, as indicated by the stability of amphibole and local partial melting, which is cross-cut by relatively undeformed N–S- to NW–SE-trending leucogranitic dikes (Fig. 2c–e). Ongoing non-coaxial deformation subsequent to dike injection is indicated by the contorted shape of some dikes (Fig. 2c and d), and by the folding of the foliation of the mylonitic xenoliths, due to heterogeneous deformation around dikes that were rotated synthetically during the general dextral shear regime (Fig. 2e).

3. The Cabanas Granite

3.1. Within-pluton petrography and structures

The Cabanas Granite is a gray, medium- to coarse-grained, equigranular two-mica leucogranite with only slight variations in grain-size (3–6 mm), modal composition and color. The granite contains less than 10 vol.% of muscovite + biotite, with muscovite commonly dominant over biotite, and subequal amounts of plagioclase (albite/oligoclase), K-feldspar (orthoclase inverted to microcline) and quartz. Porphyritic texture, with sparse K-feldspar megacrysts up to 3 cm long, is locally found. Internal contacts are rare and, where observed, they are relatively sharp and in some cases define tight folds with NE–SW trending subvertical axial planes and NE-plunging axes.

The shear zones that cross-cut and bound the Cabanas Granite to the north (Fig. 1) are characterized by pervasive solid-state deformation and show well-developed dextral *S–C* fabrics (Fig. 3a). The dominant foliation (*S*-plane) steeply dips to the northwest or southeast and *C*-planes are subvertical and have EW-strikes (Fig. 1). Some outcrops show conjugate shear bands, dextral with EW to ENE strikes, and sinistral with NE strikes. Pegmatite dikes parallel to the mylonitic foliation are cross-cut by *C*-type shear bands (Fig. 3b), suggesting that regional strike-slip shearing continued until the late magmatic stage of the pluton. Close to the shear zones, solid-state deformation evidenced by elongate quartz grains is still observed, but further away a grain shape preferred orientation is barely, if at all, discernible, and the granite looks as if it were not deformed in the solid state.

Truncation of folds and mylonitic fabrics by the Cabanas Granite indicates that it was emplaced after the foliation-forming event in the wall rocks took place and while the regional strike-slip regime was established. Synmagmatic folds and conjugate shear bands with opposed shear senses suggest that a NW–SE directed shortening was added to the overall transcurrent shearing during crystallization and cooling of the pluton. The Cabanas Granite was therefore emplaced and deformed under the same transpressive conditions reflected in the country rocks. NW–SE-trending granite dikes in the country rocks (Fig. 2) are inferred to trace the direction of maximum shortening. Absence of chilled margins in the granite and absence of contact metamorphic aureole in the country rocks point to relatively high regional temperatures during intrusion. This inference is reinforced by the microstructures present in deformed samples of the Cabanas Granite (see below).

3.2. Microstructures

In the field, a penetrative solid-state foliation commonly appears close to the shear zones that bound or cross-cut the Cabanas Granite and shows a transition to typical *S–C* fabrics within the shear zones. Away from these regions, thin-sections of the apparently isotropic, unfoliated Cabanas Granite show that subsolidus deformation features, whose intensity varies from minor to strong, is present in most

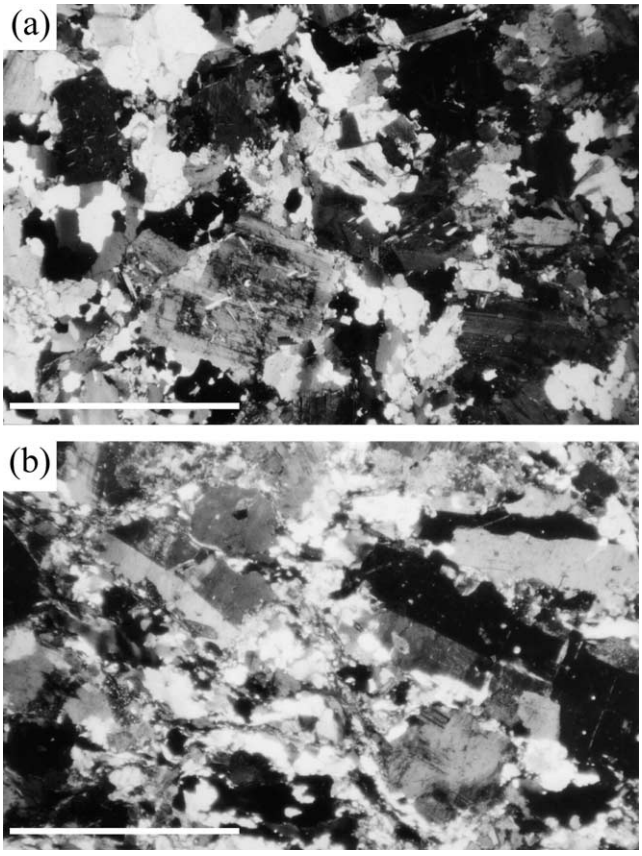

Fig. 4. (a) Photomicrograph of dominantly magmatic microstructure in the Cabanas Granite characterized by subhedral zoned crystals of plagioclase that exhibit a slight shape preferred orientation. A weak solid-state overprint is indicated by bend twin lamellas in plagioclase (lower right corner) and undulose extinction of rounded quartz grains. (b) Incipient gneissic fabric characterized by K-feldspar porphyroclasts whose largest crystal face is subparallel to the foliation plane defined by aggregates of slightly elongate quartz grains. Scale bar is 3 mm.

places. Based on detailed thin-section studies, four microstructural types were distinguished:

1. *Magmatic to high-temperature solid-state*. This microstructural type is characterized by little recrystallization of usually strain-free feldspar grains, by large quartz grains, and by the stability of biotite (Fig. 4a). Quartz may show chessboard extinction, indicating deformation at temperatures close to the granite solidus (Mainprice et al., 1986; Kruhl, 1996), or recrystallization to subgrains meeting at triple junctions. Myrmekitic intergrowths are common in some samples but rare in others. A shape preferred orientation of plagioclase grains is present in some samples. Two samples display retrogression of biotite to chlorite and sericitization of feldspars, indicating low-temperature alteration probably under static conditions.
2. *Low-strain, high-temperature solid-state*. Dynamic recrystallization of quartz to large subgrains is well advanced, feldspars show incipient to moderate recrystallization around their edges, and biotite is stable. Chessboard extinction is still common in quartz and myrmekite is abundant. Flattened quartz grains and slightly elongate aggregates of new grains are present, but continuous layers of weak minerals are not developed.
3. *Gneissic, high-temperature solid-state*. This is the high-strain equivalent of the above type. The microstructure is characterized by a shape preferred orientation of recrystallized quartz and muscovite and biotite flakes involving larger grains of feldspars (Fig. 4b). A continuum from magmatic to solid-state deformation (Paterson et al., 1989) is indicated by parallelism of albite twins of plagioclase and Carlsbad twins of K-feldspar with the long dimension of elongate grains.
4. *Gneissic, moderate-temperature solid-state*. Quartz aggregates wrap around large feldspar porphyroclasts, which may be broken and show alteration to white

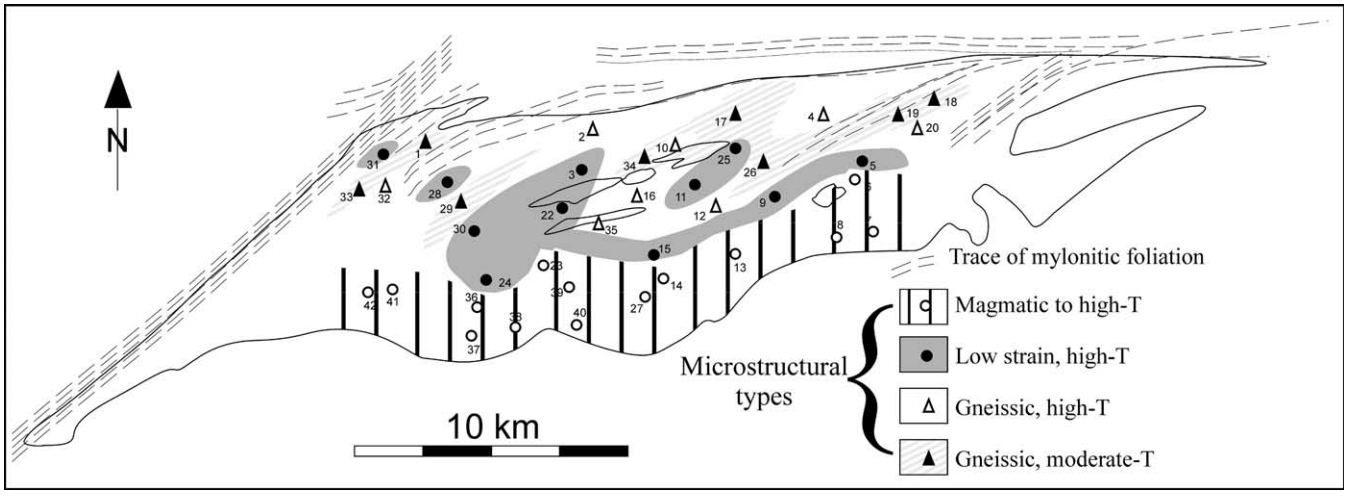

Fig. 5. Geologic sketch map of the Cabanas Granite showing microstructural domains extrapolated from locations (symbols with numbers) where samples have been analyzed.

Table 1
Anisotrophy of magnetic susceptibility database

Site	K_m (10^{-6} SI)	P' (%)	T	K_1	K_3
1	129.36	9.4	0.149	282/22	177/33
2	76.70	13.7	0.216	103/46	311/41
3	74.40	5.3	−0.041	57/79	275/9
4	52.86	10.1	0.622	249/27	153/13
5	77.96	9.2	−0.647	22/52	268/17
6	92.28	6.4	−0.850	177/16	273/24
7	67.53	6.0	−0.160	260/10	8/60
8	44.29	5.6	−0.461	4/21	228/63
9	51.76	8.4	−0.093	47/14	263/73
10	78.16	6.1	0.878	312/69	170/17
11	100.12	10.0	0.108	264/2	173/9
12	72.04	5.6	0.599	316/57	85/22
13	62.31	6.0	−0.003	321/36	138/53
14	73.40	15.7	0.989	308/27	170/55
15	70.38	7.6	0.648	70/23	195/53
16	61.24	6.6	−0.017	264/36	161/17
17	90.77	8.2	−0.105	247/45	135/21
18	75.76	9.2	0.132	64/31	328/9
19	65.87	8.8	0.472	63/51	308/19
20	91.07	9.3	0.093	58/18	167/44
21	91.48	6.2	−0.062	82/31	240/57
22	76.82	4.9	0.553	348/23	172/67
23	86.27	12.3	0.735	304/24	206/17
24	63.72	11.9	0.719	252/72	31/14
25	80.15	11.4	0.501	173/10	276/51
26	66.06	12.9	0,.222	132/9	287/80
27	76.45	9.3	0.418	273/22	174/21
28	74.21	7.9	−0.101	259/10	169/1
29	109.96	7.8	−0.012	90/53	234/32
30	60.30	6.6	0.107	1/84	201/6
31	71.31	14.4	0.679	1/7	106/66
32	76.82	5.8	0.547	273/19	46/63
33	65.00	10.4	0.297	196/10	78/70
34	68.82	6.2	−0.771	244/29	131/35
35	130.69	7.3	0.561	227/37	129/10
36	92.98	7.0	0.684	268/31	154/35
37	48.44	6.1	0.722	241/13	141/37
38	79.03	9.8	0.903	280/26	178/24
39	87.00	6.5	0.560	38/39	177/43
40	90.31	11.0	0.389	262/18	150/49
41	63.36	5.4	−0.150	61/26	162/23
42	105.53	6.8	0.007	353/47	147/40
43	70.80	8.3	−0.270	209/12	354/76
44	71.55	10.6	0.034	256/24	93/57
45	83.04	4.1	−0.379	87/60	334/13
46	67.53	6.9	0.108	337/61	83/9
47	85.47	3.3	0.278	84/14	348/23
48	55.58	3.2	−0.161	234/43	353/27
49	67.70	4.5	0.027	244/35	69/55
50	81.62	9.8	0.050	39/46	131/1
51	64.26	5.7	0.481	214/29	31/61
52	104.45	5.0	−0.208	272/36	119/51
53	90.33	6.3	0.578	178/6	75/63
54	147.35	5.6	0.238	73/32	228/55
55	72.52	8.7	0.230	276/8	17/55
56	73.10	6.4	0.265	314/72	183/12
57	56.73	5.5	−0.402	68/20	185/50
58	96.12	5.3	0.413	53/37	149/8
59	88.70	9.2	0.005	36/45	151/23

mica, and chloritization of biotite varies from incipient to moderate. Chessboard extinction is still present in some large quartz grains. Myrmekite, where present, is finer-grained than in the other microstructural types. Exsolution of perthite is common in K-feldspar. Mica fishes and microscopic *S–C* fabrics may be present and are consistent with dextral shear. Typical core-and-mantle structures and flame-perthite are absent, indicating deformation above 500 °C (Passchier and Trouw, 1996).

Moderate to strong undulose extinction observed in some quartz grains in all of the above microstructural types is probably due to late incipient superimposed strain at low temperature.

The distribution of the four microstructural types, based on 41 thin-sections from sites sampled for AMS, is shown in the map of Fig. 5. The southern half of the Cabanas Granite is characterized by dominantly magmatic or subsolidus deformation fabrics developed at low strain. Gneissic fabrics developed at moderate temperature concentrate close to the shear zones while gneissic, high-T fabrics are symmetrically disposed along them and their prolongation.

4. Anisotropy of magnetic susceptibility study

4.1. Sampling and measurements

Anisotropy of magnetic susceptibility (AMS) is particularly well adapted for the study of granites, like the Cabanas Granite, that usually have weak mineral shape-preferred orientations. In this work, 59 stations were studied for AMS. In each site, two to three 2.5-cm-diameter cores were drilled and saw-cut into two to three specimens 2.2 cm in length. The specimens were analyzed using a Kappabridge KLY3 (AGICO) susceptometer, whose resolution is better than 10^{-8} SI, at the Laboratório Helmo Rand (Universidade Federal de Pernambuco, Recife). Each specimen was measured in 15 directions, allowing the calculation of the three principal axes of the AMS ellipsoid $K_1 \geq K_2 \geq K_3$. For each site, the bulk susceptibility K was obtained by the average of the arithmetic means of the K_1, K_2, K_3 magnitudes of the specimens ($(K_1 + K_2 + K_3)/3$). To describe the degree of anisotropy and shape of the AMS ellipsoids, the P' and T parameters of Jelinek (1981) were calculated for the different AMS stations after correction for the diamagnetic component K_{dia} (estimated to be in the order of -14×10^{-6} SI; Borradaile and Henry, 1997). P' is noted in percentage ($P'\% = (P' - 1) \times 100$) in Table 1. The magnetic lineation (parallel to K_1) and foliation (normal to K_3) for each station were computed from the averages of the K_1 and K_3 orientations of individual specimens.

4.2. Bulk susceptibility and compositional zonation

Most sites (88%) have bulk susceptibilities below 10^{-4} SI (Table 1), suggesting a dominant paramagnetic character for

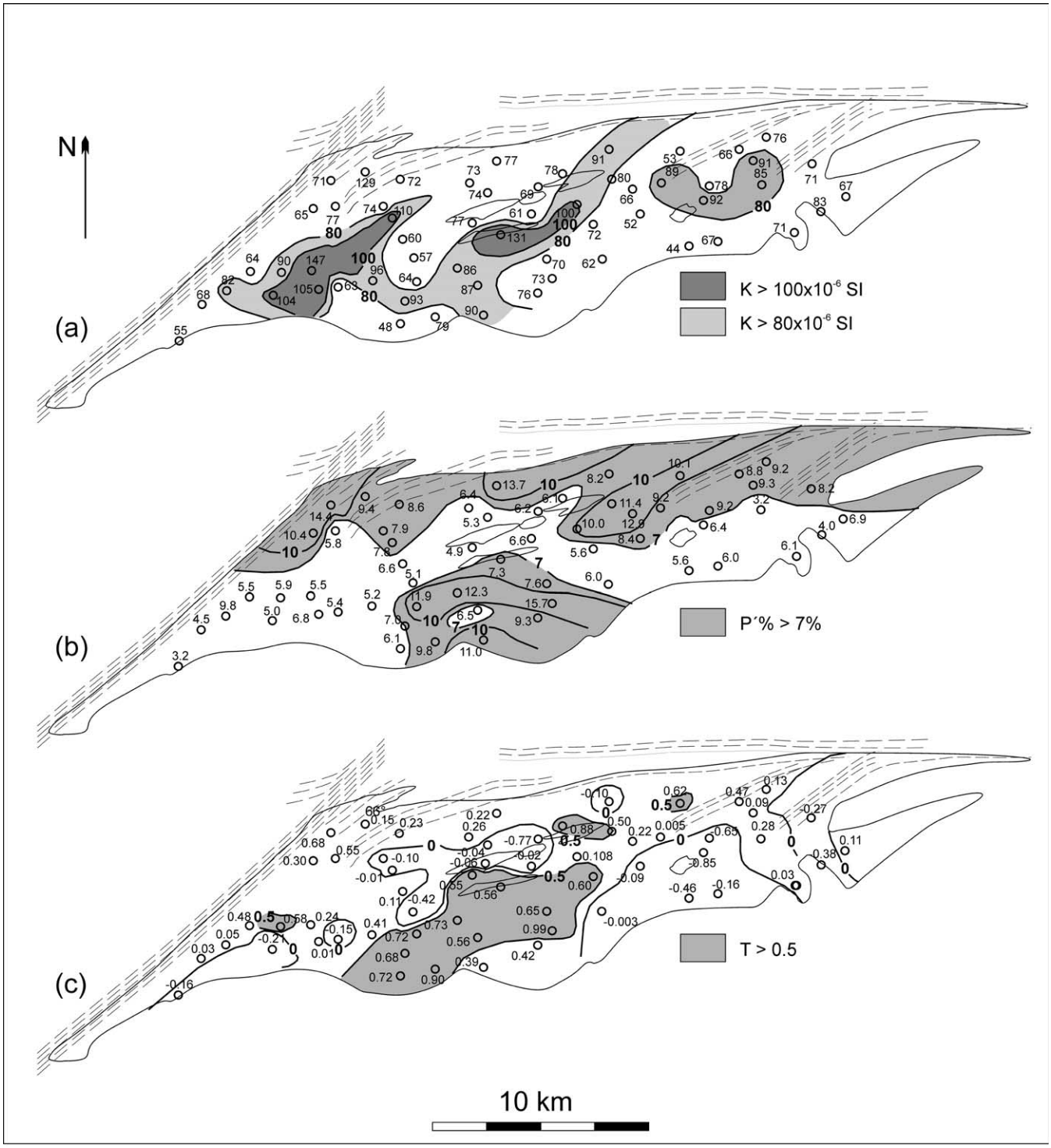

Fig. 6. Magnetic susceptibility magnitude (a), magnetic anisotropy (b) and shape parameter (c) maps of the Cabanas Granite. Lines of iso-susceptibilities (in μSI), and isovalues of P' (%) and T are manually interpolated. Dashed lines: traces of mylonitic foliation.

the Cabanas Granite. In paramagnetic granites, the iron-bearing silicates mainly carry the susceptibility, thus the distribution of K values may reveal the existence of a petrographic zonation in plutons (Gleizes et al., 1993). In the Cabanas Granite, muscovite dominates over biotite in most sites. Although muscovite may contain some iron and contribute to the bulk susceptibility, the higher iron content of biotite implies its correlation with higher susceptibility values. The contoured map of K values (Fig. 6a) shows a well-organized pattern. Its most outstanding feature is the existence of two NE–SW trending elongate zones of high susceptibilities (grayished area in Fig. 6a), one crossing

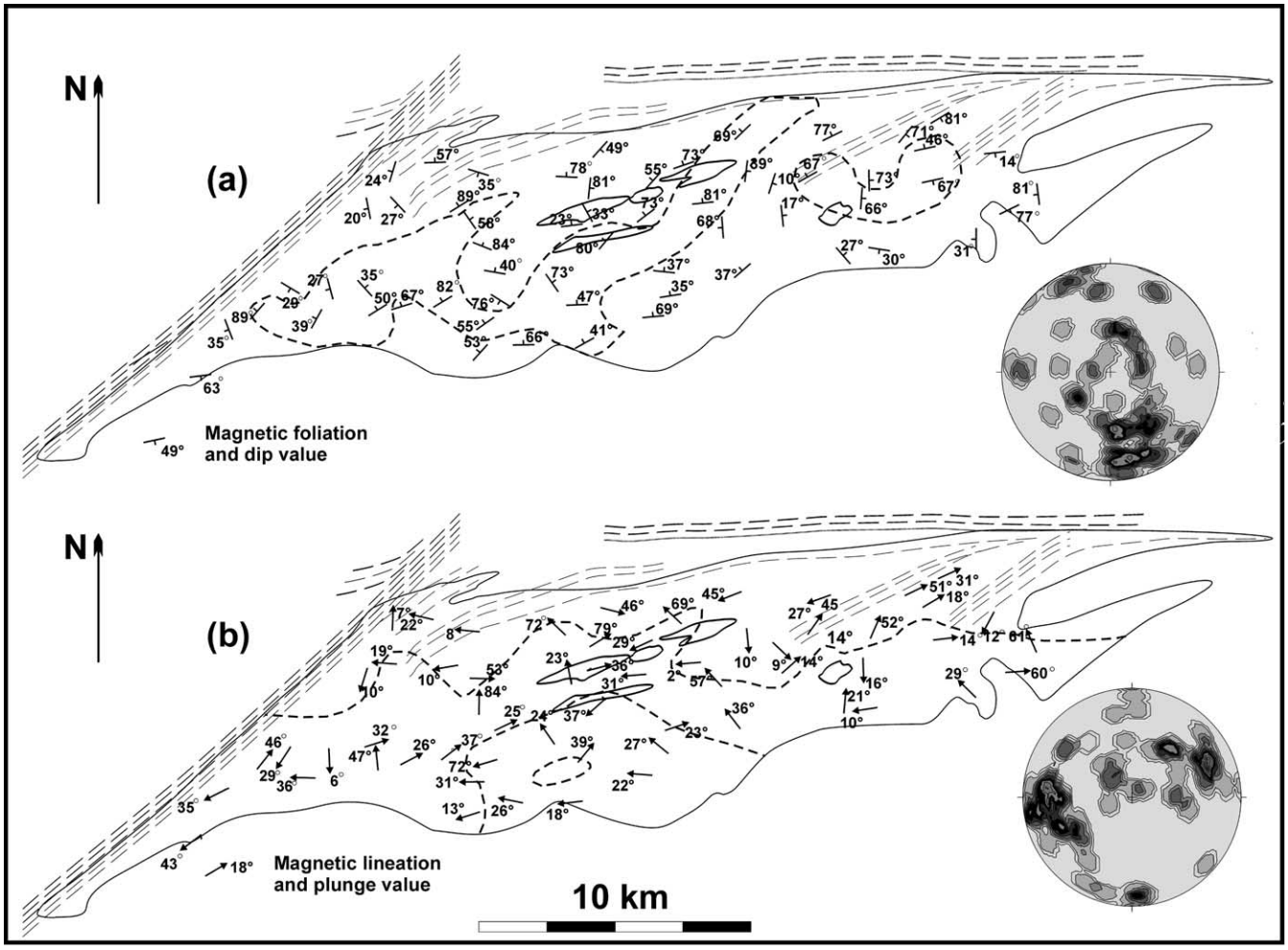

Fig. 7. Magnetic foliation (a) and lineation (b) maps of the Cabanas Granite. Stereograms are lower hemisphere Schmidt projections of contoured poles to foliation planes and lineations. Dotted lines correspond, respectively, to contour values of $K = 80 \times 10^{-6}$ SI (a) and $P' = 7\%$ (b) given in Fig. 6. Dashed lines: traces of mylonitic foliation.

the entire pluton in its central region and other one in its eastern region.

4.3. Anisotropy and shape of the AMS ellipsoids

Anisotropy values are relatively low (5–15%; Table 1) and within typical values reported for paramagnetic granites (Bouchez, 1997). The highest anisotropies (Fig. 6b) are found along the northern border, coinciding with the proximity to the strike-slip shear zones, and in the south of the pluton. In between these two regions, an E–W elongate central domain has anisotropies generally below 7%. The large xenoliths of country rock belong to areas of low anisotropies.

The T parameter shows that the majority of AMS ellipsoids have triaxial to strongly oblate shapes (Table 1), with only six stations displaying values smaller than -0.2. The geographical distribution of these shapes is, however, not random (Fig. 6c). The most remarkable features are (a) alternating ENE-trending elongate regions of triaxial to prolate and oblate ellipsoids, and (b) a region of highly oblate ellipsoids ($T > 0.5$) in the southern central part of the pluton.

4.4. Magnetic foliation and lineation

Orientations of the magnetic foliation and lineation are shown in maps and in Schmidt projections in Fig. 7. The directional data reveal two distinct patterns. Of the 59 sites sampled for AMS, 40 of them (68%) have EW- to NE-trending lineations with dominantly low to moderate plunges (less than 45° in 34 stations). The second family of structures, found in 19 sites (32%), comprises lineations with N- to NW-trends and plunges varying from subhorizontal to subvertical, dominantly towards north. This set of structures has anisotropies less than 7% in 12 sites whereas, for the first family, P' values below 7% are only found in seven stations (Fig. 7b).

The foliation of the first family has either strikes trending EW to NE and moderate to high dips (> 45° in 24 sites), or

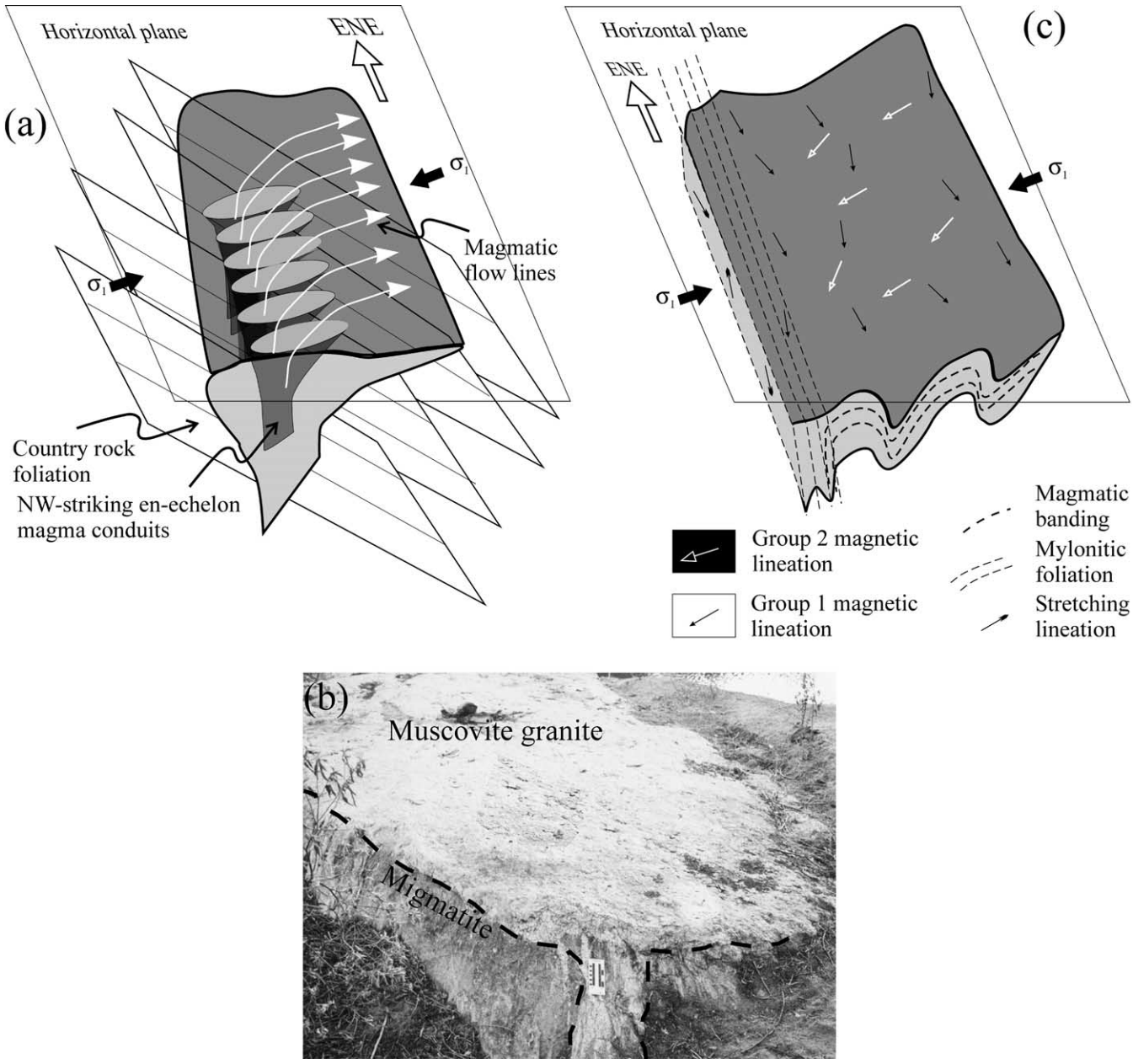

Fig. 8. Interpretative emplacement and deformation model of Cabanas Granite. (a) Magma emanating from NW–SE-striking conduits fills a subhorizontal magma chamber discordant with the moderately dipping foliation of country rocks. Arrow heads indicate sense of magma flow. (b) Horizontal sheet of granite truncating migmatite banding. The tabular granite body is fed by a subvertical dike. The situation is thought to represent a natural analogue of the model shown in (a). (c) Deformation during the late stages of crystallization led to development of magmatic shear zones and folds. Continuing strain localization during cooling gives rise to solid-state shear zones.

shows variable strikes associated with generally low dips. In the first situation, the magnetic fabric is concordant with the solid-state fabric of the shear zones that bound or cross-cut the pluton. In the second situation, they occur dominantly parallel to the *K* isovalue lines that outline fold-like structures in the central southern part of the pluton. This subset of structures is responsible for the closed girdle elongated in the NE direction seen in the stereographic plot of the poles to the magnetic foliation (Fig. 7a). The foliations of the second family have variable strikes and dips, but there is a dominance of steep dips in the north and shallow dips in the south.

5. Discussion

The eastern portion of the Borborema province is characterized by an early episode of non-coaxial shear, with a top-to-the-NE sense of displacement and development of a regional flat-lying foliation (Neves et al., 2000). This event

was followed by a more localized deformation episode during which transcurrent shear zones were developed, and by the intrusion of the large Caruaru–Arcoverde batholith (Fig. 1). Dextral strike-slip shearing along the southern margin of the Caruaru–Arcoverde batholith was synchronous with displacement along NE-trending sinistral shear zones inside the pluton. The transcurrent regime was coeval with the development of NE-trending folds in the country rocks. This behavior has been interpreted as due to strain partitioning during transpression caused by NW–SE bulk shortening (Neves and Mariano, 1999).

Xenoliths of both mylonite and folded migmatite in the Cabanas Granite (Fig. 2) prove that strike-slip shear zones and folds were already nucleated in the country rocks prior to pluton intrusion. The occurrence of outcrop-scale, conjugate dextral and sinistral shear bands in the Cabanas Granite attests the persistence of the regional transpressive regime during and after its crystallization. Taking into account this regional and local tectonic context, the AMS data acquired for the Cabanas Granite is discussed below in order to evaluate the interplay between emplacement and regional deformation.

5.1. Origin and significance of the AMS fabrics

The dominant pattern of magnetic structures (group A) in the Cabanas Granite consists of ENE-trending lineations with shallow to moderate plunges. In the north, foliations with moderate to steep dips belong to sites showing the imprint of moderate- to high-temperature solid-state fabrics (compare Figs. 5 and 7). In this part of the pluton, the observed continuum between magmatic and solid-state microstructures (Fig. 4) suggests that deformation started in the magmatic stage. In turn, this suggests that strain localization took place along shear corridors inside the pluton that initiated during magma crystallization in a regional dextral shear regime.

In the central and southern parts of the Cabanas Granite, group A structures are dominantly magmatic, with incipient superimposed high-temperature solid-state microstructures (Figs. 5 and 7). Several observations suggest that they resulted from folding due to the NW–SE regional contraction. First, the axes and axial planes of local folds of the magmatic banding have the same orientation as in outcrop- and regional-scale folds of the country rocks. Second, the symmetrical distribution of regions of relatively high- and low-susceptibility magnitudes (Fig. 6a) outlines a pattern that may be explained by the folding of a tabular pluton displaying a subhorizontal banding. Third, the presence of flattened AMS ellipsoids (Fig. 6c), high anisotropies (Fig. 6b) and moderate to shallow dipping foliations (Fig. 7a) in the south of the Cabanas Granite suggests that an initial planar subhorizontal fabric was steepened. Finally, the presence in the central and south parts of the pluton of both prolate magnetic ellipsoids (Fig. 6c) and ENE-trending lineations (Fig. 7b) is compatible with stretching parallel to the fold axes.

Group A fabrics are interpreted here as resulting from a transpression. Strain partitioning resulted in dominantly horizontal stretching of the magma parallel to the shearing direction in the northern region of the pluton, and synchronous NW shortening in its central southern part. Group B fabrics are characterized by dominant magmatic or low-strain, high-temperature microstructures (Figs. 5 and 7). The lineations of this group have consistent NW trends and their plunges vary from subvertical to subhorizontal. Their development cannot be readily explained in terms of regional deformation. Instead, the dominance of magmatic microstructures and relatively low anisotropy degrees in most sites suggest that these structures were developed during the emplacement of the pluton. The variations in lineation plunges suggest lateral flows away from magma upwelling zones, as if the pluton was fed through NW–SE-oriented conduits.

5.2. Emplacement and deformation of the Cabanas Granite

The proposed model for emplacement of the Cabanas Granite takes into account: (a) the regional tectonic framework given by the country rocks; (b) the internal structure of the pluton; (c) the existence of NW-trending leucogranite dikes cutting the country rocks; and (d) the three-dimensional shape of outcrop-scale intrusions of muscovite granites observed to the south of the study area.

In transpression, the intermediate principal stress may become horizontal with decreasing depth (see Brown and Solar, 1998). This favors emplacement of tabular intrusions. Accordingly, the group B magnetic structures in the Cabanas Granite may reflect the lateral spreading of a flat-lying magma chamber filled by en échelon NW-oriented fractures (Fig. 8a). An outcrop-scale analogue of this mechanism is shown in Fig. 8b, where a horizontal sheet of granite is fed by a large vertical dike. Since lacolith formation is unlikely to happen at depths below approximately 3 km (Roman-Berdiel et al., 1995) and emplacement of the Cabanas Granite does not seem to have imposed any significant lateral strain on its walls, the pluton may have grown by floor depression (Cruden, 1998). The final geometry of the pluton before its post-emplacement deformation is therefore viewed as being that of an asymmetric lopolith thicker in the north than in the south, accounting for the overall NW-plunge of the magnetic lineations of group B (Fig. 8a).

The interpreted original subhorizontal foliation was affected by post-emplacement, synmagmatic to solid-state deformation leading to folds and shear bands (Fig. 8c). The large xenoliths observed in the pluton may represent in situ fragments of country rock that were engulfed by the growing magma chamber. Another possibility is that they represent windows located in the core of antiformal folds where pluton's floor may outcrop. Persistent strain during

cooling of the Cabanas Granite was likely at the origin of corridors of *S–C* mylonites outside of which the early formed structures could be preserved.

5.3. Emplacement fabric versus regional fabric imprint

The AMS technique is now a well established tool in the structural study of plutonic rocks, having been applied successfully to dozens of cases in the last two decades. Magnetic foliations and lineations have been mainly used to infer emplacement mechanisms or as markers of regional deformation. They are interpreted either as reflecting the kinematics of magma deformation at its site of emplacement (e.g. Tobisch and Cruden, 1995; Aranguren et al., 1997; McNulty et al., 2000), or as indicating the direction of finite strain to which the magma was subjected during regional deformation (e.g., Neves et al., 1996; Benn et al., 1998).

The internal structure of the Cabanas Granite, which would never have been pictured without the help of the magnetic fabrics, reveals the existence of both syn-emplacement fabrics produced by flow related to magma transport, and post-emplacement fabrics due to the effect of regional deformation. Clearly, during syntectonic emplacement, emplacement-related magmatic fabrics are not likely to be preserved in the case of crystal-poor magmas. This suggests that the magma which originated the Cabanas Granite reached the emplacement site containing a considerable proportion of crystals.

Once settled in its emplacement site, the crystallization time delay of a pluton depends on the difference between the magma temperature and its solidus temperature (Vauchez et al., 1997; Paterson et al., 1998), the volume of the intrusion, the country rock temperature, and if the system was open or closed. High-level plutons, expected to crystallize rapidly, will preferentially display emplacement-related fabrics. This has been suggested for tabular bodies fed by en échelon conduits like the Dinkey Creek and Bald Mountain plutons in the central Sierra Nevada batholith (Tobisch and Cruden, 1995), and the Los Pedroches batholith in Spain (Aranguren et al., 1997). These plutons were emplaced in low-grade metamorphic rocks, rapidly cooling and preserving their emplacement fabrics. On the other hand, plutons emplaced in high-*T* environments, especially if fed by high-temperature magmas, should largely reflect regional strain (Neves et al., 1996; Vauchez et al., 1997; Benn et al., 1998). The Cabanas Granite represents the intermediate situation of a tabular pluton formed by crystallization of low-temperature melts emplaced in a moderately warm crust, preserving both emplacement and regional deformation fabrics.

The above considerations suggest that plutons with such composite fabrics should be more common. Composite fabrics may have simply been overlooked in the case where one pattern predominates with respect to the other.

Acknowledgements

This work was supported by grants from the *Conselho Nacional de Desenvolvimento CientÍfico e Tecnológico* of Brazil. We thank B. Davis for his comments and discussion, J.-L. Bouchez for thorough and constructive reviews on earlier versions of the manuscript, and J. Hippertt for editorial advice.

References

Améglio, L., Vigneresse, J.-L., Bouchez, J.-L., 1997. Granite pluton geometry and emplacement model inferred from combined fabric and gravity data. In: Bouchez, J.-L., Hutton, D.H.W., Stephens, W.E. (Eds.). Granite: From Segregation of Melt to Emplacement Fabrics. Kluwer Academic Publishers, pp. 199–214.

Aranguren, A., Larrea, F.J., Carracedo, M., Cuevas, J., TubÍa, J.M., 1997. The Los Pedroches Batholith (southern Spain): polyphase interplay between shear zones in transtension and setting of granites. In: Bouchez, J.-L., Hutton, D.H.W., Stephens, W.E. (Eds.). Granite: From Segregation of Melt to Emplacement Fabrics. Kluwer Academic Publishers, pp. 215–229.

Archanjo, C.J., Bouchez, J.-L., Corsini, M., Vauchez, A., 1994. The Pombal granite pluton: magnetic fabric, emplacement and relationships with the Brasiliano strike-slip setting of NE Brazil (Paraiba State). Journal of Structural Geology 16, 323–335.

Benn, K., Ham, N.M., Pignotta, G.S., Bleeker, W., 1998. Emplacement and deformation of granites during transpression: magnetic fabrics of the Archean Sparrow pluton, Slave Province, Canada. Journal of Structural Geology 20, 1247–1259.

Borradaile, G.J., Henry, B., 1997. Tectonic applications of magnetic susceptibility and its anisotropy. Earth Science Reviews 42, 49–93.

Bouchez, J.-L., 1997. Granite is never isotropic: an introduction to AMS studies of granitic rocks. In: Bouchez, J.-L., Hutton, D.H.W., Stephens, W.E. (Eds.). Granite: From Segregation of Melt to Emplacement Fabrics. Kluwer Academic Publishers, pp. 95–112.

Bouchez, J.-L., Gleizes, G., 1995. Two-stage deformation of the Mont-Louis-Andorra granite pluton (Variscan Pyrenees) inferred from magnetic susceptibility anisotropy. Journal of the Geological Society, London 152, 669–679.

Brown, M., Solar, G.S., 1998. Granite ascent and emplacement during contractional deformation in convergent orogens. Journal of Structural Geology 20, 1365–1393.

Corsini, M., Lambert de Figueiredo, L., Caby, R., Feraud, G., Ruffet, G., Vauchez, A., 1998. Thermal history of the Pan-African/Brasiliano Borborema Province of northeast Brazil deduced from $^{40}Ar/^{39}Ar$ analysis. Tectonophysics 285, 103–117.

Cruden, A.R., 1998. On the emplacement of tabular granites. Journal of the Geological Society, London 155, 853–862.

Ferré, E., Gleizes, G., Bouchez, J.-L., 1995. Internal fabric and strike-slip emplacement of the Pan-African granite of Solli Hills, northern Nigeria. Tectonics 14, 1205–1219.

Gleizes, G., Nédélec, A., Bouchez, J.-L., Autran, A., Rochette, P., 1993. Magnetic susceptibility of the Mont-Louis Andorra ilmenite-type granite (Pyrenees): a new tool for the petrographic characterization and regional mapping of zoned granite plutons. Journal of Geophysical Research 98, 4317–4331.

Gleizes, G., Leblanc, D., Santana, V., Olivier, P., Bouchez, J.-L., 1998. Sigmoidal structures featuring dextral shear during emplacement of the Hercynian granite complex of Cauterets–Panticosa (Pyrenees). Journal of Structural Geology 20, 1229–1245.

Guimarães, I.P., Almeida, C.N., Da Silva Filho, A.F., Araújo, J.M.M., 2000. Granitoids marking the end of the Brasiliano (Pan-African)

orogeny within the Central Tectonic Domain of the Borborema province. Revista Brasileira de Geociências 30, 177–181.

Hutton, D.H.W., 1982. A tectonic model for the emplacement of the Main Donegal Granite, NW Ireland. Journal of the Geological Society, London 139, 615–631.

Jelinek, V., 1981. Characterization of the magnetic fabrics in rocks. Tectonophysics 79, 63–67.

Kruhl, J.H., 1996. Prism- and basal-plane parallel subgrain boundaries in quartz: a microstructural geothermobarometer. Journal of Metamorphic Geology 14, 581–589.

Mainprice, D., Bouchez, J.-L., Blumenfeld, P., Tubiá, J.M., 1986. Dominant c slip in naturally deformed quartz: implications for dramatic plastic softening at high temperature. Geology 14, 819–822.

McCaffrey, K.J.W., 1992. Igneous emplacement in a transpressive shear zone: Ox Mountains igneous complex. Journal of the Geological Society, London 149, 221–235.

McNulty, B.A., Tobish, O.T., Cruden, A.R., Gilder, S., 2000. Multistage emplacement of the Mount Givens pluton, Central Sierra Nevada batholith. Geological Society of America Bulletin 112, 119–135.

Neves, S.P., Mariano, G., 1999. Assessing the tectonic significance of a large-scale transcurrent shear zone system: the Pernambuco lineament, northeastern Brazil. Journal of Structural Geology 21, 1369–1383.

Neves, S.P., Vauchez, A., Archanjo, C.J., 1996. Shear-zone controlled magma emplacement or magma-assisted nucleation of shear zones? Insights from northeast Brazil. Tectonophysics 262, 349–365.

Neves, S.P., Vauchez, A., Feraud, G., 2000. Tectono-thermal evolution, magma emplacement, and shear zone development in the Caruaru area (Borborema Province, NE Brazil). Precambrian Research 99, 1–32.

Passchier, C.W., Trouw, R.A.J., 1996. Microtectonics. Springer-Verlag, Berlin.

Paterson, S.R., Vernon, R.H., Tobish, O.T., 1989. A review of criteria for identification of magmatic and tectonic foliations in granitoids. Journal of Structural Geology 11, 349–363.

Paterson, S.R., Fowler Jr., T.K., Schmidt, K.L., Yoshinobu, A.S., Yuan, E.S., Miller, R.B., 1998. Interpreting magmatic fabric patterns in plutons. Lithos 44, 53–82.

Roman-Berdiel, T., Gapais, D., Brun, J.P., 1995. Analogue models of laccolith formation. Journal of Structural Geology 17, 1337–1346.

Silva, J.M.R., Mariano, G., 2000. Geometry and kinematics of the Afogados da Ingazeira shear zone, Northeast Brazil. International Geology Review 42, 86–95.

Tobisch, O.T., Cruden, A.R., 1995. Fracture-controlled magma conduits in an obliquely convergent continental magmatic arc. Geology 23, 941–944.

Vauchez, A., Egydio-Silva, M., 1992. Termination of a continental-scale strike-slip fault in partially melted crust: the West Pernambuco shear zone, northeast Brazil. Geology 20, 1007–1010.

Vauchez, A., Neves, S.P., Caby, R., Corsini, M., Egydio-Silva, M., Arthaud, M.H., Amaro, V., 1995. The Borborema shear zone system, NE Brazil. Journal of South America Earth Sciences 8, 247–266.

Vauchez, A., Neves, S.P., Tommasi, A., 1997. Transcurrent shear zones and magma emplacement in Neoproterozoic belts of Brazil. In: Bouchez, J.-L., Hutton, D.H.W., Stephens, W.E. (Eds.). Granite: From Segregation of Melt to Emplacement Fabrics. Kluwer Academic Publishers, pp. 275–293.

Vigneresse, J.-L., Bouchez, J.-L., 1997. Successive granitic magma batches during pluton emplacement: the case of Cabeza de Araya (Spain). Journal of Petrology 38, 1767–1776.

Yenes, M., Alvarez, F., Gutiérrez-Alonso, G., 1999. Granite emplacement in orogenic compressional conditions: the La Alberca-Béjar granite area (Spanish Central System, Variscan Iberian Belt). Journal of Structural Geology 21, 1419–1440.